PERGAMON

Organic Geochemistry 32 (2001) 633–645

Organic Geochemistry

www.elsevier.nl/locate/orggeochem

Identification of a novel alkenone in Black Sea sediments

L. Xu [a,b], C.M. Reddy [a], J.W. Farrington [a], G.S. Frysinger [c], R.B. Gaines [c], C.G. Johnson [a], R.K. Nelson [a], T.I. Eglinton [a,*]

[a] *Department of Marine Chemistry and Geochemistry, Woods Hole Oceanographic Institution, Woods Hole, MA 02543, USA*
[b] *Environmental Science Research Center, Xiamen University, Xiamen, Fujian 361005, China*
[c] *Department of Science, US Coast Guard Academy, New London, CT 06320, USA*

Received 17 February 2000; accepted 8 February 2001
(returned to author for revision 11 April 2000)

Abstract

We report the identification of a novel long-chain ketone in Holocene Black Sea sediments. Based on chemical properties, and chromatographic and mass spectrometric characteristics, this compound has been identified as a di-unsaturated C_{36} ethyl ketone. Further analyses indicated the position and configuration of the double bonds, and the novel alkenone was determined to be hexatriaconta-(16*E*,21*E*)-dien-3-one. While this compound is present in only trace quantities in Unit I sediments, it is the most abundant alkenone in portions of Unit II. Its presence thus apparently pre-dates the invasion of *Emiliania huxleyi* in the Black Sea. The down-core profiles and isotopic compositions suggest that the precursor for the $C_{36:2}$ alkenone may be distinct from that of the $C_{37\text{-}39}$ alkenones, however the biological origin of this novel compound is presently unknown.

Keywords: Alkenone; Structure characterization; Sediment; Black Sea; Holocene; Haptophytes

1. Introduction

Long-chain (C_{37}, C_{38} and C_{39}) unsaturated methyl and ethyl ketones (alkenones) were first discovered in sediments from Walvis Ridge off West Africa by Boon et al. (1978) and later fully characterized by de Leeuw et al. (1980), Volkman et al. (1980a) and Rechka and Maxwell (1988a,b). These compounds have been found to be characteristic of haptophyte microalgae, including the cosmopolitan coccolithophorid *Emiliania huxleyi* (Volkman et al., 1980b), which first appeared in the late Pleistocene. This species is considered to be the dominant source of these compounds encountered in most contemporary marine sediments. These compounds are of great interest to paleoceanographers (Eglinton et al., 2000) because of their use as proxies for past sea surface temperatures (e.g. Brassell et al., 1986; Prahl and Wakeham, 1987; Farrington et al., 1988; McCaffrey et al., 1990; Eglinton et al., 1992) and partial pressures of CO_2 (Jasper and Hayes, 1990; Jasper et al., 1994). As a result, these remarkable compounds are now amongst the most extensively studied class of lipids in marine organic geochemistry.

The general structure of the alkenones is unusual. In particular, the *trans* (*E*) geometry of the double bonds is distinct from most non-conjugated polyunsaturated lipid natural products, which as a rule have double bonds with *cis* (*Z*) geometry. Their biosynthesis has not been investigated, although there have been suggestions that it may be related to fatty acids (Volkman et al., 1980a; Marlowe et al., 1984). Some biosynthetically-related compounds such as alkenes (de Leeuw et al., 1980; Volkman et al., 1980a) and alkyl alkenoates (Marlowe et al., 1984b; Conte et al., 1998) have also been reported in algae and marine sediments. There is little knowledge of the physiological function of these compounds.

* Corresponding author. Tel.: +1-508-289-2627; fax: +1-508-457-2164.
E-mail address: teglinton@whoi.edu (T.I. Eglinton).

0146-6380/01/$ - see front matter
PII: S0146-6380(01)00019-5

Here we report the identification of a new alkenone from Black Sea sediments, and compare its structural and isotopic characteristics to those of the C_{37} counterparts that are more commonly observed.

2. Experimental

2.1. Sediment samples

Black Sea sediments from one box core and a giant gravity core were investigated in this study. These cores were collected from the central western basin in May 1988 during Leg 1 of the R/V Knorr cruise 134 (for additional details, see Jones and Gagnon, 1994). The box core (BC-17) was collected at 42°58′N, 31°25′E at a water depth of 2066 m. It was sub-sampled using PVC tubing which recovered sediment from the surface to ~58 cm depth. The sediment sub-core was split vertically and then stored below −20°C until analysis. The giant gravity core (GGC-19, core length 2.5 m) was collected at 42°53′N, 31°23′E at a water depth of 2096 m. The core tube (PVC pipe) was sectioned at 1.5 m intervals, split vertically, and then stored at 4°C until analysis. Prior to sectioning, both cores were brought to room temperature, and various sediment sections (1–3 cm in thickness) were air-dried at room temperature before analysis.

2.2. Reference materials

A purified sample of heptatriaconta-(15*E*,22*E*)-dien-2-one ($C_{37:2}$ alkenone) was isolated from a 20 l culture of the marine haptophyte *Isochrysis galbana*. The seed culture was grown under continuous light at 20°C in filtered (1 μm, GF/F) deep Sargasso seawater (1000 m) supplemented with f/2 vitamins, and was harvested when it reached stationary phase. The cells were collected on GF/F filters (1 μm, 90 mm), homogenized, and extracted with hexane/dichloromethane (4:1). A ketone fraction was separated from the raw lipids by thin layer chromatography (TLC) using silica gel G plates (Macherey–Nagel) developed in hexane. The mixed alkenone band was scraped off the plate, re-suspended in hexane, centrifuged to remove the silica, and loaded onto a second silica gel G plate which was developed using hexane/acetone (85:15). A band corresponding to the $C_{37:2}$ alkenone was recovered and determined to be chromatographically pure (>90%) based on gas chromatographic and mass spectrometric analysis.

Two authentic fatty acid standards, octadec-(9*E*)-enoic acid (elaidic acid) and octadec-(9*Z*)-enoic acid (oleic acid), were purchased (Aldrich) and used as is.

2.3. Bulk analyses

An aliquot of the dried, homogenized sample was treated with 10% HCl to remove any carbonates. The carbonate-free sediment was analyzed for total organic carbon (TOC) content with a Carlo Erba 1108 elemental analyzer. The stable carbon isotope ratio ($\delta^{13}C$) and the radiocarbon abundance (^{14}C age) of the TOC was measured on purified CO_2 after the carbonate-free sediment was combusted in the presence of CuO. The $\delta^{13}C$ was determined by isotope ratio mass spectrometry and ^{14}C content by accelerator mass spectrometry (AMS) after conversion of the CO_2 to graphite (McNichol et al., 1994). Precision is about ±0.1 ‰ and ± ~80 years for $\delta^{13}C$ and ^{14}C age measurements, respectively.

2.4. Lipid extraction and separation

Sediment samples (between 0.5 and 20 g dry wt.) were extracted by pressurized fluid extraction (Dionex ASE-200) using dichloromethane and methanol (9:1, v/v; 100° C, 1000 psi) (Sessions et al., 1999). Extracts were taken to dryness under a stream of N_2 and saponified using 2 M KOH in methanol-water (4:1 v/v; 10 ml, 80°C, 2 h). The products were extracted three times with dichloromethane-hexane (1:4 v/v) after the addition of 10% sodium chloride in distilled water (10 ml). The combined extracts were brought to dryness under a stream of N_2, re-dissolved in hexane/ether (95:5, v/v), and deposited on top of a small glass column (15 cm × 4 mm I.D.) containing fully-activated silica gel (100–200 mesh). Compounds were eluted with hexane/ether (95:5, v/v, 15 ml, hydrocarbon fraction) followed by dichloromethane/hexane (40:60, v/v, 60 ml, alkenone fraction).

For selected samples, the alkenone fraction was further separated and purified with a combination of urea adduction, reverse phase high-pressure liquid chromatography (HPLC), and Ag^+ SiO_2 column chromatography. The urea adduction was performed as described by Marlowe et al. (1984a). The alkenones, which were contained in the urea-adducted fraction, were then separated by isocratic HPLC on a Supelco LC-18 column (250 × 4.6 mm, 3 μm) with acetonitrile/dichloromethane (82:18, v/v, 28°C) as the eluent (1.5 ml/min). Five percent of the column flow was diverted to a SEDEX 55 evaporative light scattering detector (ELSD) using a T-splitter. Five fractions were collected according to detector response. The F_2 fraction contained the new alkenone and the $C_{38:3}$ methyl and ethyl alkenones (Fig. 1).

The F_2 fraction from HPLC was further separated with Ag^+ SiO_2 column chromatography. The Ag^+ SiO_2 was prepared by mixing the silica gel (100–200 mesh; 80 g) with silver nitrate (16 g) in 200 ml of methanol/H_2O (4:1; v/v). The slurry was dried and activated in the dark at 120°C overnight. Glass columns (same size as above) were packed with the Ag^+ SiO_2 and charged with the F_2 fraction from HPLC. The new alkenone was eluted with diethyl ether/hexane (40:60, v/v, 30 ml) and the triunsaturated $C_{38:3}$ ethyl and methyl alkenones were eluted with 100% diethyl ether.

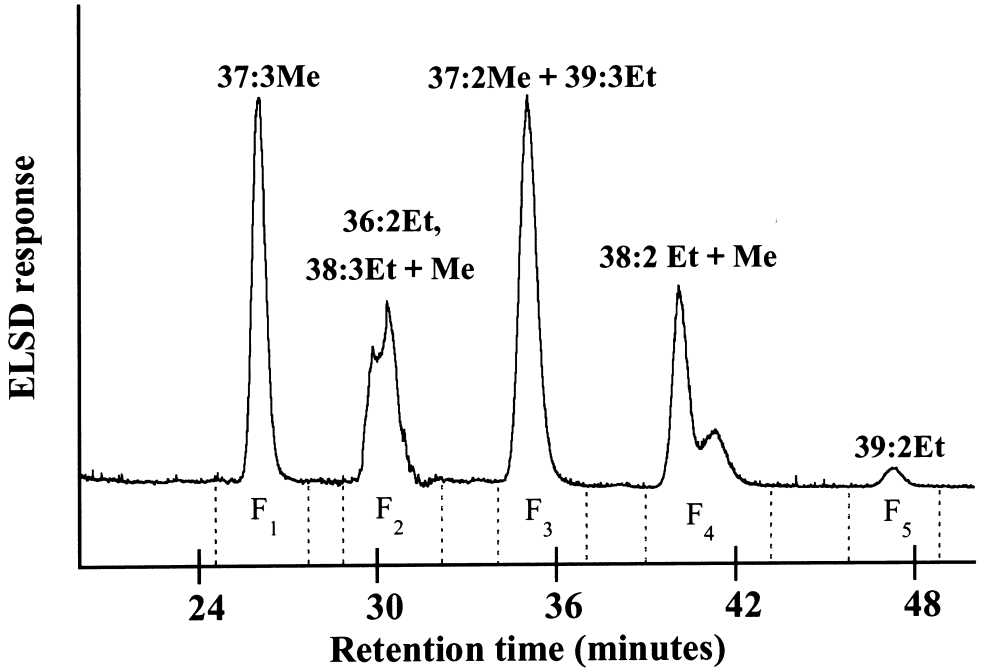

Fig. 1. HPLC-ELSD chromatogram of a urea-adducted alkenone fraction. F_1–F_5 fractions are labeled accordingly and the dotted lines define each fraction. Alkenones present in each fraction are listed. The new compound is labeled 36:2Et.

2.5. Gas chromatography (GC)

Alkenone-containing fractions were analyzed on a Hewlett Packard (HP) 5890 II Plus GC fitted with a PTV injector (Gerstel), a dual column inlet splitter and two FID detectors. Using this configuration, simultaneous separation of components was achieved on a CP-Sil5-CB (Chrompack) and Rtx-200 (Restek) (both columns were 60 m × 0.32 mm I.D., 0.25 μm film thickness). The GC oven was programmed from 40°C (1 min), at 20°C/min to 220°C and then at 2°C/min to 320°C, and held at the final temperature for 15 min. Helium was used as the carrier gas in the constant flow mode, with an initial pressure of 110 kPa at 40°C.

2.6. Comprehensive two-dimensional gas chromatography (GC×GC)

Comprehensive two-dimensional gas chromatography (Phillips and Beens, 1999; Bertsch, 2000) was performed using a Zoex GC×GC system. This consisted of an HP 6890 GC configured with a split injector, thermal modulator assembly for analyte transfer between two serially connected columns, and an FID (Phillips et al., 1999). The first dimension separation was performed on a nonpolar polydimethylsiloxane phase (007-1, Quadrex, 9.5 m × 0.10 mm I.D., 0.5 μm film thickness) and temperature programmed from 220 to 320°C at 2.5°C/min (15 min hold at maximum temp.). The modulation capillary was polydimethylsiloxane (0.08 m × 0.10 mm I.D., 0.5 μm film thickness) and temperature programmed from 200 to 290°C at 2.5°C/min with a 19 min hold. The second dimension separation was performed on a polar trifluoropropylmethyl phase (Rtx-200, Restek, 1.0 m × 0.10 mm I.D., 0.1 μm film thickness) held at 320°C for the entire analysis time (55 min). Column sections between heated zones were interconnected using segments of deactivated fused silica column with glass press-fit connectors. Hydrogen was used as the carrier gas in constant flow mode (0.4 ml/min). The thermal modulator was maintained 100°C above the temperature of the modulator capillary. The heater rotated at 0.25 rev/s over the modulator capillary column to desorb trapped analyte and inject it into the second-dimension column. Second-dimension injections occurred every 2.5 s.

2.7. Gas chromatography–infrared spectroscopy (GC–IR) and fourier transform–infrared spectroscopy (FT–IR)

Alkenones were analyzed by GC–IR on a Bourne Scientific infrared chromatograph. Compounds were injected in splitless mode, and separated on a DB-5 capillary column (10 m × 0.25 mm ID) using a temperature program from 110 to 300°C at 20°C/min (15 min hold at final temp.). The eluent stream was sprayed onto a cooled, moving ZnSe window. The carrier gas

was pumped away under vacuum and the data station collected a continuous array of IR spectra (4000–650 cm^{-1}) off the ZnSe window.

Conventional FT–IR spectra were acquired on a Nicolet 510P spectrometer. The purified alkenone was dissolved in dichloromethane, applied to a NaCl plate and the solvent allowed to evaporate. Signal was accumulated over 64 scans (4000–600 cm^{-1}).

2.8. Gas chromatography–mass spectrometry (GC–MS)

For compound identification, electron impact (EI) spectra were acquired on a HP 6890 gas chromatograph connected to a HP 5973 mass selective detector. Compounds were separated on a DB-5 (J&W) glass capillary column (60 m × 0.32 mm I.D., 0.25 μm film thickness). The oven temperature was programmed from 40 to 240°C at 20°C/min and then to 320 at 1°C/min and then held for 20 min. The carrier gas (He) pressure was 28 kPa at 40°C. The source temperature was 230°C and the electron energy was 70 eV. Spectra were acquired between m/z 40-650 at a scan rate of 1 cycle s^{-1}.

2.9. Probe-mass spectrometry

Accurate mass measurement of the molecular ion region of the new compound was obtained using a Micromass Autospec-Q mass spectrometer. Approximately 150 ng of the compound were loaded onto the platinum wire loop of a modified direct exposure probe and volatilized by resistively heating the loop from 0 to 1.5 A at a rate of 1.5 A/min (Eglinton et al., 1996; Johnson et al., 1997). The mass spectrometer source was operated in EI mode at 185°C and 70 eV. The spectrometer was tuned to greater than 15,000 resolution and voltage scans were performed from m/z 491 to 533. Data were acquired in continuum mode and analyzed using the OPUS software package.

Aliquots of the new alkenone (in 50 μl hexane) were treated with dimethyl disulfide (DMDS, 100 μl) and an iodine solution in ether (60 mg/ml, 30 μl) in a 2 ml vial (40°C for 20 h) (Leonhardt and DeVilbiss, 1985). After cooling to room temperature and dilution with hexane (0.2 ml), the iodine was deactivated by shaking with a 5% aqueous solution of $Na_2S_2O_3$ (0.5 ml). The organic phase was removed and the aqueous phase extracted with hexane. The combined hexane solution was dried with Na_2SO_4, concentrated under a N_2 stream to about 50 μl and subsequently stored at 4°C. The double bond positions were determined by direct insertion (probe) MS (Finnigan MAT Voyager 8000) of the DMDS adducts. The DMDS adducts were loaded on the platinum wire loop of the direct insertion probe. The probe temperature was raised from 30 to 200°C in 10 min. The spectra were recorded in EI mode at 70 eV, scanning from m/z 50 to 800 with a cycle time of 1 s.

2.10. Isotope ratio monitoring gas chromatography–mass spectrometry (irm-GC–MS)

Stable carbon isotopic analyses of individual alkenones were performed on a Hewlett Packard 6890 GC interfaced to a modified Finnigan GC Combustion III unit and a Finnigan Delta^{Plus} isotope mass spectrometer. Compounds were separated on a DB-5ms (J&W)

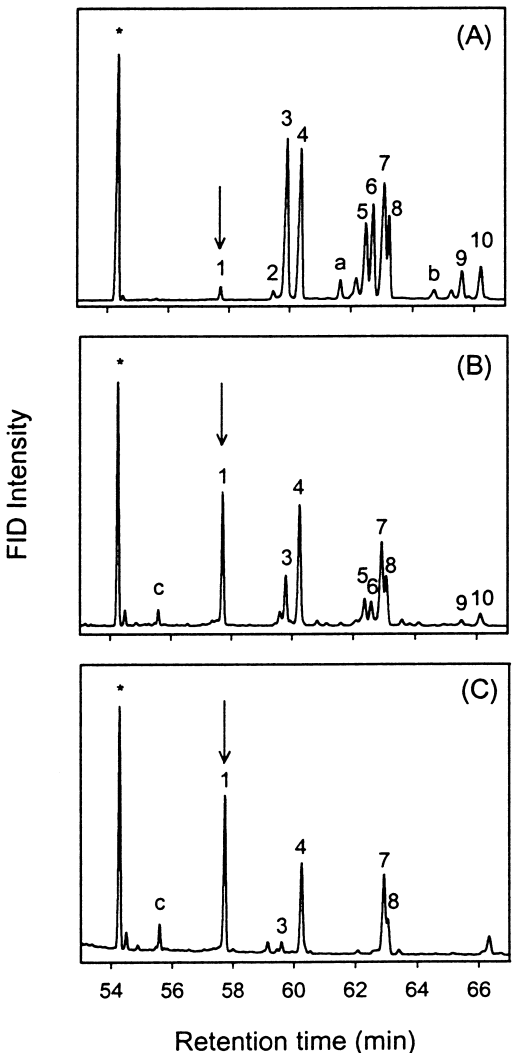

Fig. 2. Partial gas chromatograms (FID) of alkenones in sediments: Core BC-17 at (A) 3–5 cm and (B) 33–36 cm and core GGC-19 at (C) 27–28 cm. Chromatographic conditions (capillary column CP-Sil5-CB) are described in the experimental section. Peak identifications: *, n-$C_{36}H_{74}$ internal standard, 1. New compound $C_{36:2}$Et (also denoted with arrow); 2. $C_{37:4}$; 3. $C_{37:3}$Me; 4. $C_{37:2}$Me; 5. $C_{38:3}$Et; 6. $C_{38:3}$Me; 7. $C_{38:2}$Et; 8. $C_{38:2}$Me; 9. $C_{39:3}$ Et; 10. $C_{39:2}$Et. Et and Me denote ethyl and methyl ketones, respectively. Peaks labeled a, b, c are tentatively identified as $C_{38:4}$Me, $C_{39:4}$, and $C_{35:2}$Me alkenones, respectively.

capillary column (60 m × 0.32 mm I.D., 0.25 μm film thickness). During each analysis, pulses of reference CO_2 were bled into the mass spectrometer and were used for calibration relative to the Vienna Pee Dee Belemnite standard. Alkenone fractions were injected three times and the reported values are the mean value. The precision (as expressed as the standard deviation of the three injections) was no greater than 0.6 ‰ and averaged 0.25 ‰. The $\delta^{13}C$ values for coinjected n-C_{36} were within 0.5 ‰ of the actual value (as determined with standard off-line techniques).

2.11. Nuclear magnetic resonance spectrometry (NMR)

NMR experiments were performed on a Bruker Avance 400 DPX spectrometer. Spectra were acquired at either 400 MHz (^1H) or 100 MHz (^{13}C). All samples were dissolved in $CDCl_3$ (Aldrich, 100.0 atom%D) and spectra were acquired using a 5 mm broadband inverse probe and manufacturer-provided pulse sequences. Spectra were referenced to the undeuterated $CHCl_3$ impurity ($\delta = 7.28$ ppm) for ^1H or the center peak of the $CDCl_3$ triplet ($\delta = 77.41$ ppm) for ^{13}C.

3. Results and discussion

3.1. Identification of new alkenone

The elution of the new compound in the isolation scheme and the retention time of the new compound for both GC columns are consistent with a C_{36} ketone (Fig. 2). In reverse phase HPLC, the new compound coeluted with the methyl and ethyl $C_{38:3}$ alkenones ($C_{38:3}$Me and $C_{38:3}$Et, respectively; Fig. 1). The new compound eluted earlier and was completely separated from the $C_{38:3}$ alkenones by Ag^+ silica gel column chromatography, suggesting that the new compound had less than three double bonds. The EI mass spectrum of the unknown compound (Fig. 3A) yielded a prominent molecular ion (M^+) at m/z 516. The base peak (m/z 57) and the diagnostic fragment ions at M-18, M-29, M-47 and M-72 indicated a dienoic ethyl ketone, since ethyl and methyl ketones have base peaks at m/z 57 and 43, respectively (de Leeuw et al., 1980).[1] In high resolution MS, the molecular ion was found to have a mass of 516.5268 ± 0.0010 Da ($n = 4$) and the single ^{13}C isotopic molecular ion was found to have a mass of 517.5300 ± 0.0005 Da ($n = 4$). The only elemental composition consistent with these data given all possible combinations of C, ^{13}C, H, N, O, P and S was $C_{36}H_{68}O$, corresponding to a 36 carbon di-unsaturated ketone ($C_{36:2}$).

Alkenone fractions from selected intervals were analyzed by comprehensive two-dimensional gas chromatography (GC×GC; Fig. 4). The FID data are displayed as a two-dimensional image where the x-axis is first-dimension retention time, the y-axis is second-dimension retention time, and the color contour represents FID signal intensity (Gaines et al., 1999). The x-axis is a volatility-based separation, so the elution order of the alkenones is the same as observed in the one-dimensional GC trace (Fig. 2A–C), whereas the y-axis in the GC×GC chromatogram represents a polarity-based separation. n-Alkanes (the n-C_{36} internal standard and traces of n-C_{37} and n-C_{38} as impurities) represent the least polar components, and are distributed across the bottom of the chromatogram. The trifluoropropyl methyl stationary phase exhibits selectivity towards ketone functional groups, and has been shown as an effective complement to apolar stationary phases in two-dimensional GC of alkenones (Thomsen et al., 1998).

The well-known $C_{37:3}$Me, $C_{37:2}$Me, $C_{38:3}$Et, $C_{38:3}$Me, $C_{38:2}$Et, $C_{38:2}$Me, $C_{39:3}$Et, and $C_{39:2}$Et alkenones are identified based on their first dimension elution order (Fig. 4). Analysis of the positions of the peaks corresponding to these compounds indicates that they are organized into two distinct bands. The methyl alkenones are slightly more polar and form a band of components (labeled "Me") above and approximately parallel to the ethyl alkenones (labeled "Et"). This systematic grouping of classes of related chemical components is one of the significant advantages of comprehensive two-dimensional gas chromatography (Gaines et al., 1999). The $C_{36:2}$ alkenone, which elutes on the ×-axis between the n-C_{37} and n-C_{38} alkanes, intersects the "Et" line on the second dimension (Fig. 4), lending further support to the notion that is it an ethyl ketone.

By virtue of the higher selectivity and sensitivity of GC×GC (Phillips et al., 1999), a number of additional components of equivalent volatility and polarity to the alkenones are also apparent in Fig. 4. Moreover, the information contained in the GC×GC chromatogram provides constraints on the chemical characteristics of these unknown compounds. In particular, the grouping into the methyl- and ethyl-alkenone bands provides insights into their likely structures. Based on this information, the $C_{35:2}$Me, $C_{37:4}$Et, $C_{37:1}$Me, $C_{38:4}$Me, $C_{38:1}$Et and $C_{39:4}$Et alkenones are tentatively identified (Fig. 4, see also Fig. 2). Mass spectral characteristics (M^+, base peak from GC–MS analysis) of the more abundant of these unknowns (i.e. $C_{35:2}$Me, $C_{37:1}$Me, $C_{38:1}$Et, and $C_{39:4}$Et) support these interpretations.

Mass spectrometry of the corresponding DMDS adduct of the new compound was used to deduce the locations of the two double bonds (Leonhardt and DeVilbiss, 1985). The resulting mass spectrum indicates

[1] N.B. Some long-chain alkenes synthesized by *Emiliania huxleyi* yield similar mass spectra and exhibit similar retention times to the $C_{36:2}$ alkenone (de Leeuw et al., 1980; Volkman et al., 1980b).

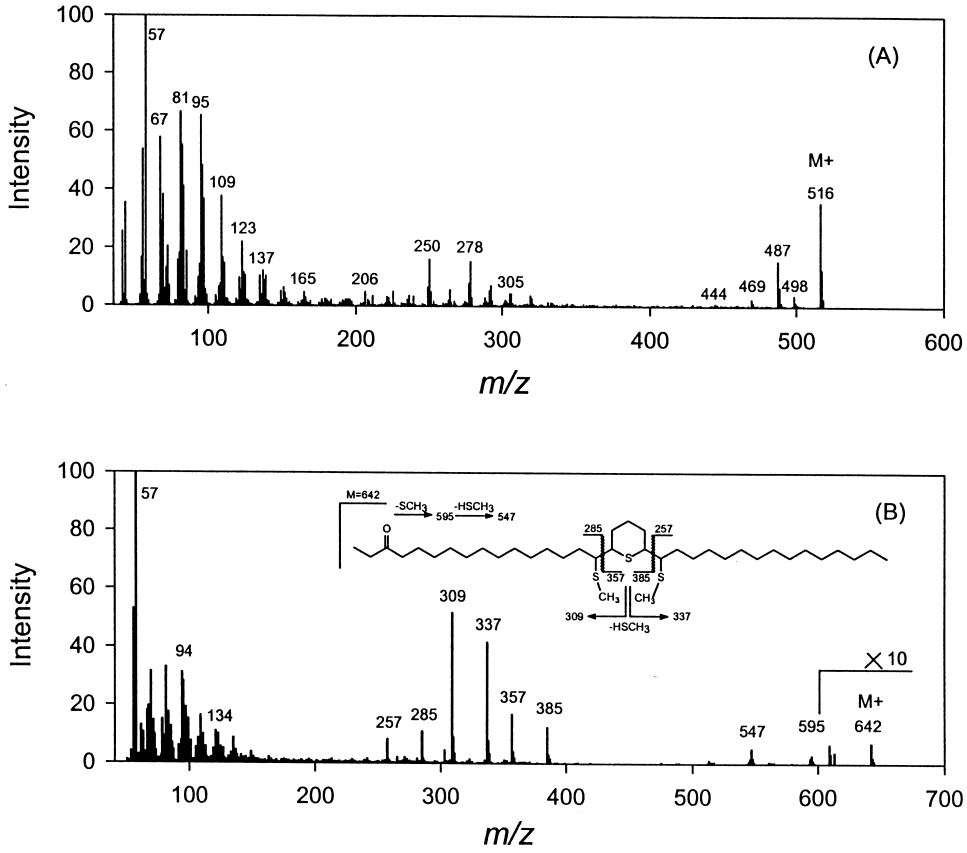

Fig. 3. The EI mass spectrum of the new compound (A). The mass spectrum of the DMDS adduct of the new compound (B). Proposed assignments for fragment ions are indicated on the structure (inset).

the double bond positions at carbon number 16 and 21 (Fig. 3B), as revealed by diagnostic fragment ions (*m/z* 257, $C_{16}H_{33}S$ and *m/z* 285, $C_{17}H_{33}OS$) corresponding to cleavage between the two pairs of methylthio groups. All other major fragmentation can be explained by a hexa-ring formation between the two pairs of the methylthio groups (Fig. 3B).

The relative proportions of the new compound to other (known) alkenones remained unchanged after urea adduction. This suggests that the new compound has the same double bond configuration as other alkenones (i.e. *trans*; Rechka and Maxwell, 1988a) since compounds with *trans* double bonds are more likely to be adducted than compounds with *cis* double bonds (Christie, 1982).

A series of NMR experiments were performed to confirm the positions and stereochemistry of the double bonds. Results were compared with those from identical experiments performed on the purified $C_{37:2}$Me alkenone and unsaturated fatty acid standards, as well as NMR results reported by Rieley et al. (1998) for long-chain alkenes in haptophyte algae.

The ^{1}H NMR spectra of both the $C_{36:2}$ (Fig. 5) and the $C_{37:2}$ alkenone show a multiplet at 5.40 ppm. For comparison, the protons around the double bond of *cis*- and *trans*- 9-octadecenoic acid have double bond resonances of 5.37 and 5.40 ppm respectively, providing further evidence for a *trans* (*E*) geometry in the new compound. The integrated area of four hydrogens corresponding to the two double bonds in positions 16 and 21. The 5.40 ppm multiplet was shown to be coupled to an eight hydrogen multiplet at 1.99 ppm using a ^{1}H–^{1}H COSY experiment. Thus, the 1.99 ppm signal corresponds to the hydrogens on the four carbons at positions 15, 18, 20 and 23 which are alpha to the double bonds. The same COSY experiment indicated a coupling between the 1.99 ppm multiplet and a multiplet at 1.43 ppm. The area of the 1.43 ppm signal identifies this as the two hydrogens on carbon 19.

Selective decoupling experiments (1D ^{1}H sequence with homodecoupling) confirm the above assignments and allow further analysis of the 1.99 ppm multiplet as the sum of multiplets at 2.00 ppm and 1.98 ppm corresponding to the hydrogens on carbons 18 and 20 and carbons 15 and 23, respectively.

Decoupled ^{13}C spectra were obtained for the $C_{36:2}$ alkenone. DEPT experiments were used to determine

the hybridization of carbons observed in the ^{13}C NMR spectrum. An inverse ^{1}H–^{13}C correlation (hetcorr) experiment was used to assign the sp^3 ^{13}C signals at 33.02 and 32.43 ppm to carbons 15 and 23 and carbons 18 and 20, respectively. Decoupled ^{13}C spectra were also obtained for the $C_{37:2}$ alkenone, and *trans*- and *cis*-

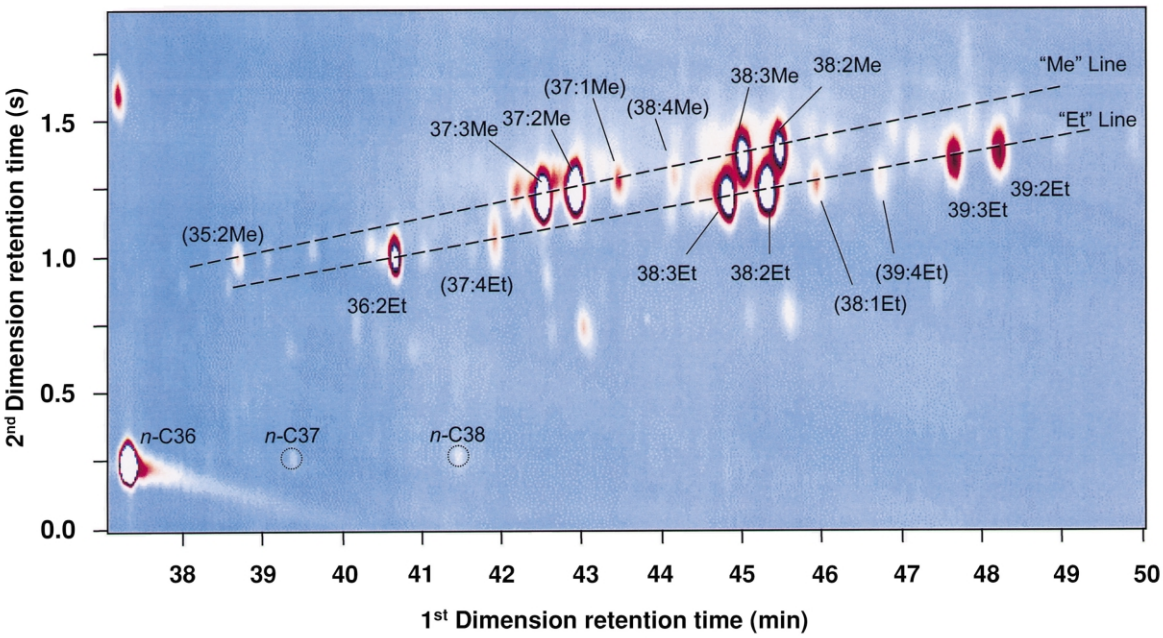

Fig. 4. Partial GC×GC chromatogram of alkenones in Black Sea sediments (Core BC-17, 3–5 cm). Peaks corresponding to $C_{37:3}$Me, $C_{37:2}$Me, $C_{38:3}$Et, $C_{38:3}$Mt, $C_{38:2}$Et, $C_{38:2}$Me, $C_{39:3}$Et, and $C_{39:2}$Et alkenones are identified. Dashed lines indicate chromatographic ordering of ethyl- ("Et") and methyl- ("Me") alkenones. The new $C_{36:2}$Et alkenone peak, intersects the "Et" Line. Additional novel alkenones tentatively identified (shown in parentheses): $C_{35:2}$Me, $C_{37:4}$Et, $C_{37:1}$Me, $C_{38:4}$Me, $C_{38:1}$Et, and $C_{39:4}$Et.

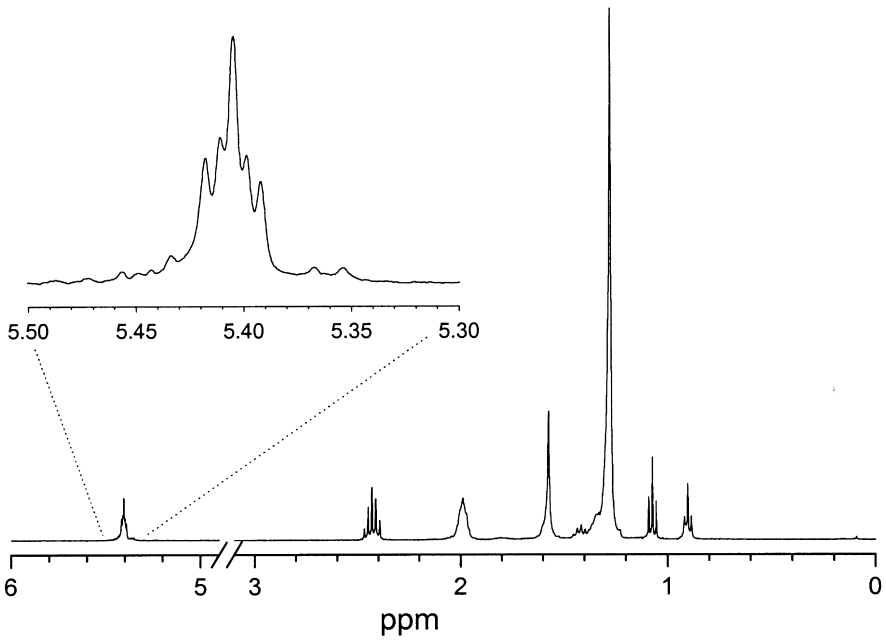

Fig. 5. ^{1}H NMR spectrum of the new $C_{36:2}$ alkenone. Inset shows expanded region of the spectrum between 5.3 and 5.5 ppm.

9-octadecenoic acid. The shifts of the carbons alpha to the double bonds were determined to be 33.01 and 32.96 ppm for the alkenone, 33.01 and 32.95 ppm for the *trans*- fatty acid, and 27.62 ppm and 27.56 ppm for the *cis*- fatty acid. Batchelor et al. (1974) have documented a 5 ppm upfield shift for the carbons alpha to the double bond in *cis*- as compared with *trans*-9-octadecenoic acid.

Taken together, the results from these NMR experiments confirm that each of the double bonds in the $C_{36:2}$ alkenone have the *trans* geometry. The appearance of carbons 18 and 20 at 32.43 ppm rather than 32.96 ppm for carbons 17 and 21 in the $C_{37:2}$ alkenone is attributed to effects of the shorter chain length between the two double bonds in this compound.

Finally, analysis of the new compound and the $C_{37:2}$ alkenone by GC–IR (Fig. 6) and FT–IR (not shown) yielded spectra that were very similar to one another and to that reported by Rechka and Maxwell (1988a) for a synthetic all-*E* $C_{37:3}$ alkenone. In particular, the characteristic band at 962 cm^{-1} (C-H stretching) confirmed the presence of *trans* double bonds. Moreover, the equivalent absorption for *cis* double bonds at 695 cm^{-1} was not observed.

Based on the above results, we identify the new compound as hexatriaconta-(16*E*,21*E*)-dien-3-one (Fig. 7). The major difference between this new compound and the known alkenones is the number of carbon atoms between the double bonds. The new compound has a three carbon distance between the double bonds, whereas the double bonds in the $C_{37:2}$ and $C_{37:3}$ alkenones are separated by five carbons. No tri- or tetra-unsaturated counterpart to this molecule was observed in any of the Black Sea sediments studied, and no hydrocarbon (alkene) or ester counterparts were detected in the other lipid fractions. However, we have tentatively identified, at much smaller concentrations, several other novel alkenones in Black Sea sediments. These include $C_{35:2}$Me, $C_{37:1}$Me, $C_{38:1}$Et, $C_{38:4}$Me, and $C_{39:4}$Et alkenones (see Fig. 4). We have also reviewed most of the published chromatograms of alkenones. Only in chromatograms from the Black Sea (Freeman and Wakeham, 1992) and Qinghai Lake (Li et al., 1996) do we see peaks that may correspond to the $C_{36:2}$ alkenone.

3.2. Sedimentary record of alkenones in the Black Sea

Late Quaternary sediments of the Black Sea can be divided into three lithostratigraphic sections: Units I, II, and III (Hay et al., 1991). Unit I, the uppermost unit, is a laminated, organic carbon rich (3–7% TOC), coccolith marl, with abundant *E. huxleyi* skeletons (Arthur et al., 1994). The deepest section of Unit I documents the first invasion of *E. huxleyi* and is briefly interrupted by a transition sapropel before returning to the deposition of coccolith marl that has continued to the present day (Fig. 8A). Unit II sediments are very organic-rich (3 to 20% TOC), carbonate-poor sapropelic muds (Arthur et al., 1994). Unit III sediments are organic carbon poor

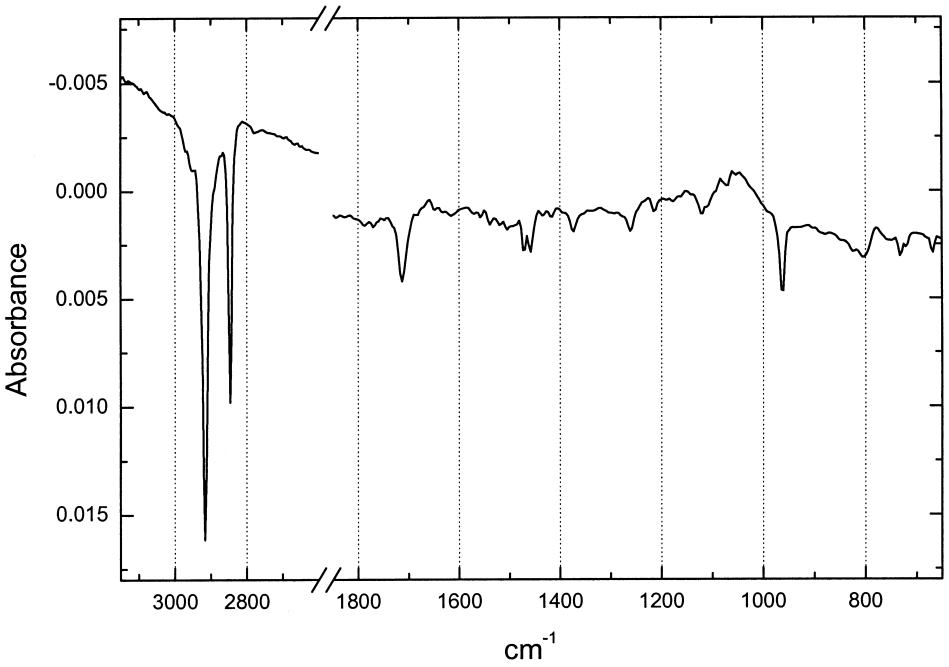

Fig. 6. Infrared spectrum (from GC–IR) of the new $C_{36:2}$ alkenone.

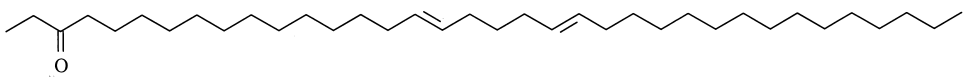

Hextriaconta-(16*E*,21*E*)-dien-3-one
($C_{36:2}$)

Fig. 7. The structure of the new compound: hexatriaconta-(16*E*,21*E*)-dien-3-one ($C_{36:2}$).

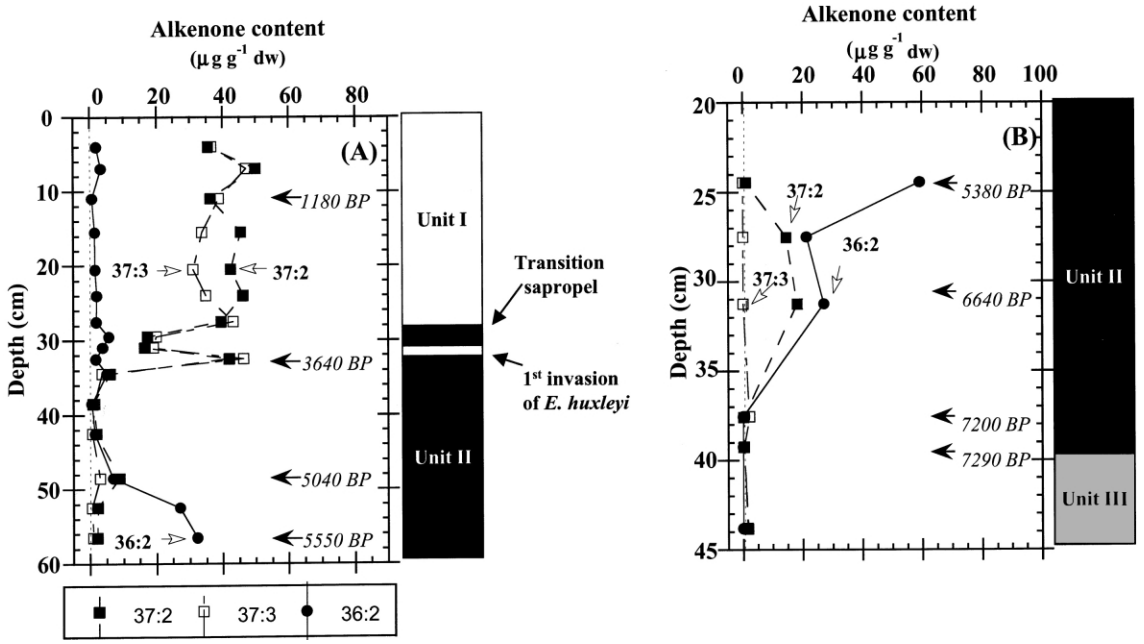

Fig. 8. The down-core concentration profiles for the $C_{36:2}$ alkenone, together with the $C_{37:2}$ and $C_{37:3}$ ketones (normalized to bulk sediment dry weight) in BC-17 (A) and GGC-19 (B). The conventional radiocarbon dates (uncorrected) are *italicized*. All of the dates are from Jones and Gagnon (1994), except for the two oldest dates in BC-17. Symbols used in Fig. 8a are the same as those in Fig. 8B.

clays (<1% TOC) (Arthur et al., 1994). The sediment chronologies shown in Fig. 8 for BC-17 and GGC-19 are conventional organic carbon ^{14}C ages obtained by Jones and Gagnon (1994). Additional samples were measured as part of this study. No reservoir correction has been applied to these dates. Based on visual analyses of BC-17, the first invasion of *E. huxleyi* is placed at 32–33 cm (~3640 ^{14}C y BP) and the transition sapropel between 28 and 32 cm, after which the remaining Unit I sediments were laid down. BC-17 did not penetrate Unit III. The upper layers of sediment were not recovered in GGC-19 and it only contains Units II and III sediments. The transition from Unit II to Unit III in GGC-19 occurs at ~39 cm (~7290 ^{14}C y BP).

Down-core profiles for the contents of $C_{36:2}$ alkenone, together with the $C_{37:2}$ and $C_{37:3}$ alkenones are shown in Fig. 8A and B for BC-17 and GGC-19, respectively. Intriguingly, the new compound displays almost a mirror image of the C_{37} counterparts in BC-17 (Fig. 8A). The abundance of $C_{36:2}$ maximizes in the sapropel portion of the BC-17 (Unit II), while the C_{37} alkenones show the highest concentrations in Unit I. This trend is also clearly evident in the transition sapropel where much lower abundances of $C_{37:2}$ and $C_{37:3}$ alkenones coincide with a significant increase of the $C_{36:2}$ alkenone (Fig. 8A).

The downcore profile of alkenones in GGC-19 slightly overlaps the record of BC-17 and then extends through Unit II and into Unit III (Fig. 8B). The concentration of $C_{36:2}$ is highest in middle section of Unit II and is barely detectable in lower Unit II and in Unit III sediments. Surprisingly, there is an increase of $C_{37:2}$ at ~26 and ~31 cm, where the concentrations approach 15 μg/g. These sediments clearly predate the invasion of *E. huxleyi* by more than 2000 ^{14}C years and suggest an alternative source of the $C_{37:2}$ alkenone. There also is a clear trend of increased saturation of alkenones with depth that appears closely tied with the lithostratigraphic units (Table 1; Figs. 2 and 8). In fact, some of the Unit II sediments are predominantly diunsaturated C_{36}–C_{39} alkenones (Fig. 2C). Alkenone-derived sea-surface temperature (SST) estimates based on the unsatura-

Table 1
The $\delta^{13}C$ values (in ‰ relative to VPDB) of alkenones and TOC in BC-17 boxcore. The standard deviations for triplicate analysis are in parentheses. Alkenone unsaturation ratios $(U^{K'}_{37})$ and corresponding estimates of past sea surface temperature (SST) are also shown

Depth (cm)	$\delta^{13}C_{TOC}$ (‰)	$\delta^{13}C_{36:2}$ (‰)	$\delta^{13}C_{37:3}$ (‰)	$\delta^{13}C_{37:2}$ (‰)	$U^{K'}_{37}$	SST[a] (°C)	Lithostratigraphic unit
6.5–7.5	−24.8	−28.0[b]	−29.3 (0.1)	−27.9 (0.1)	0.507	13.8	Unit I
10–12	−24.3	NDP[c]	−29.9 (0.1)	−27.4 (0.2)	0.464	12.5	Unit I
15–16	−24.1	NDP	−29.6 (0.2)	−27.5 (0.3)	0.568	15.6	Unit I
19.5–21.5	−24.5	NDP	−29.7 (0.4)	−27.5 (0.3)	0.573	15.7	Unit I
23.5–24.5	−24.7	NDP	−28.5 (0.4)	−26.7 (0.3)	0.562	15.4	Unit I
29–30	−25.8	NDP	−30.8 (0.5)	−27.3 (0.6)	0.648	17.9	Transition sapropel
30–32	−25.5	−28.0 (0.5)	−28.2 (0.2)	−26.5 (0.2)	0.500	13.6	Transition sapropel
32–33	−24.8	NDP	−30.2 (0.3)	−27.5 (0.3)	0.498	13.5	Invasion of E. huxleyi
33–36	−24.1	−21.0 (0.1)	−28.7 (0.1)	−25.7 (0.1)	0.664	18.4	Unit II
38–39	−25.2	−24.3 (0.4)	NDP	−27.2 (0.2)	0.715	19.9	Unit II
42–43	−25.2	−22.7 (0.2)	−31.4 (0.1)	−26.5 (0.3)	0.727	20.2	Unit II
47–50	−25.4	−23.2 (0.2)	−30.1 (0.2)	−26.5 (0.4)	0.739	20.6	Unit II
56–57	−23.5	−21.8 (0.1)	NDP	NDP	0.708	19.7	Unit II

[a] SST calculated using calibration: $U^{K'}_{37} = 0.034T + 0.039$ (Prahl et al., 1988).
[b] This compound was only measured once.
[c] NDP = no determination possible.

tion parameter, $U^{K'}_{37}$, and the calibration of Prahl et al. (1988; Table 1) suggest a large difference between Unit II (ave., 19.8°C) and Unit I (ave., 14.6°C). A shift of similar magnitude occurs between the uppermost interval of Unit II and the first invasion of *E. huxleyi*, implying dramatic fluctuations in SST on timescales of ca. 200 y (Table 1). Although there is evidence for a warmer climate in some parts of the N. hemisphere during the early Holocene, the abruptness and amplitude of these apparent SST changes suggest that other factors may be responsible for the changes in $U^{K'}_{37}$. Possibilities include diagenetic modification or different biological precursors for the $C_{37:2}$ and $C_{37:3}$ alkenones.

Some evidence exists for preferential loss of more unsaturated alkenones during oxic diagenesis (Gong and Hollander, 1999), but not for anoxic sediments. Reaction of alkenones with reduced sulfur species may occur in anoxic systems (Sinninghe Damsté et al., 1989; Schouten et al., 1993), but there is no evidence of this in Black Sea sediments (Wakeham et al., 1995). Furthermore, Koopmans et al. (1997) suggest that the sequestration of alkenones by sulfur or by oxygen linkages would probably not affect the alkenone SST index.

Stable carbon isotopic measurements may provide information on genetic relationships between the different alkenones (Freeman and Wakeham, 1992). We measured the $\delta^{13}C$ values of the $C_{36:2}$, $C_{37:3}$ and $C_{37:3}$ alkenones and of TOC for several depth horizons in BC-17 (Table 1). Relative to the TOC, the $\delta^{13}C$ values of the three alkenones were depleted by 2–5‰ in Unit I and the transition sapropel. The $\delta^{13}C$ values of the three alkenones were similar (−30.8 to −26.5‰; n = 16) but generally the $C_{37:2}$ alkenone was the most ^{13}C enriched in Unit I sediments. These $\delta^{13}C$ values are similar for those reported by Freeman and Wakeham (1992) for $C_{37:2}$ and $C_{37:3}$ alkenones in Black Sea surface sediment (0–1 cm). In contrast, the isotopic compositions of the new compound were vastly different from the C_{37} homologs in Unit II. In addition, there was significant disparity (up to 4.9‰) between the δ-values of the $C_{37:2}$ and $C_{37:3}$ alkenones in this Unit. The $C_{36:2}$ alkenone was the most enriched, with $\delta^{13}C$ values of −24.3 to −21.0‰ ($n = 5$), while the $\delta^{13}C$ values of $C_{37:2}$ and $C_{37:3}$ alkenones ranged from −31.4 to −25.7‰ ($n = 7$). Unusually, the $\delta^{13}C$ values of the $C_{36:2}$ alkenone were even more enriched in ^{13}C than the bulk TOC. Freeman and Wakeham (1992) have suggested from analyses of Black Sea particles that the $C_{37:4}$ alkenone may have a different biological source because the $\delta^{13}C$ values of the $C_{37:4}$ were independent of the more saturated isomers ($C_{37:2}$ and $C_{37:3}$). Unfortunately, the abundance was too low to measure the $\delta^{13}C$ of the $C_{37:4}$ alkenone in the sediment intervals studied here. Based on these concentration/isotopic profiles, we infer that the $C_{36:2}$ ketone has an origin that is distinct from the longer-chain ketones, and that related species may have contributed alkenones to Black Sea sediments deposited during the early Holocene.

Interestingly, there is a significant correlation ($r^2 = 0.63$) between the difference in isotopic compositions of the $C_{37:2}$ and $C_{37:3}$ alkenones (i.e. $\Delta\delta_{37:2}$–$\delta_{37:3}$) and $U^{K'}_{37}$ calculated from the relative abundance of these two alkenones (Table 1). Based on these data, we tentatively conclude that the large down-core variations in

alkenone-derived SST most likely reflect changes in contributions from different alkenone-synthesizing precursors during the evolution of the Black Sea. In such circumstances, the $U^{K'}_{37}$ parameter may not be a reliable proxy for paleo-SST.

Cross-plots of the concentrations of $C_{36:2}$, $C_{37:2}$, and $C_{37:3}$ alkenones versus sedimentary TOC for Unit I and II sediments (Fig. 9A) reveal that the $C_{36:2}$ ketone is positively correlated with TOC. While this might suggest that the precursor for the novel ketone was a major primary producer within the Black Sea, the lack of correlation between $\delta^{13}C$ values of the TOC and $C_{36:2}$ (or the other two alkenones) does not support this interpretation (Fig. 9B). Instead, the correlation of the concentrations of $C_{36:2}$ and TOC may reflect periods of increased preservation of organic matter, and/or unfavorable conditions for the deposition of biogenic carbonate (diluent).

It is interesting to further consider these results in light of the evolution of the Black Sea during the Holocene. The transitions from Unit III to Unit I reflect a series of changes driven primarily by the incursion of salt water from the Mediterranean Sea (Arthur and Dean, 1998). The system has evolved from an oxic freshwater lake (Unit III) to a moderately saline, stratified, permanently anoxic marine basin (Units I and II). After development of a sapropel following the introduction of marine waters (Unit II), a second major lithological change occurred which corresponds to the colonization of the Black Sea by *E. huxleyi* (Unit I). This invasion has been considered to represent a salinity threshold above which *E. huxleyi* populations can be sustained (Bukry, 1974). Based on this premise, we assume that the alkenones in Unit II sediments (i.e., prior to this invasion) derive from other haptophyte microalgae. The presence of alkenones in lacustrine sediments (Cranwell, 1983) clearly indicates that freshwater precursors must exist. Although lacustrine alkenones are slightly unusual because they typically contain higher degrees of unsaturation relative to those from marine samples (Cranwell, 1983; Li et al., 1996; Thiel et al., 1997), the paucity of alkenones in Unit III sediments suggests that the $C_{36:2}$ alkenone does not originate from a freshwater species.

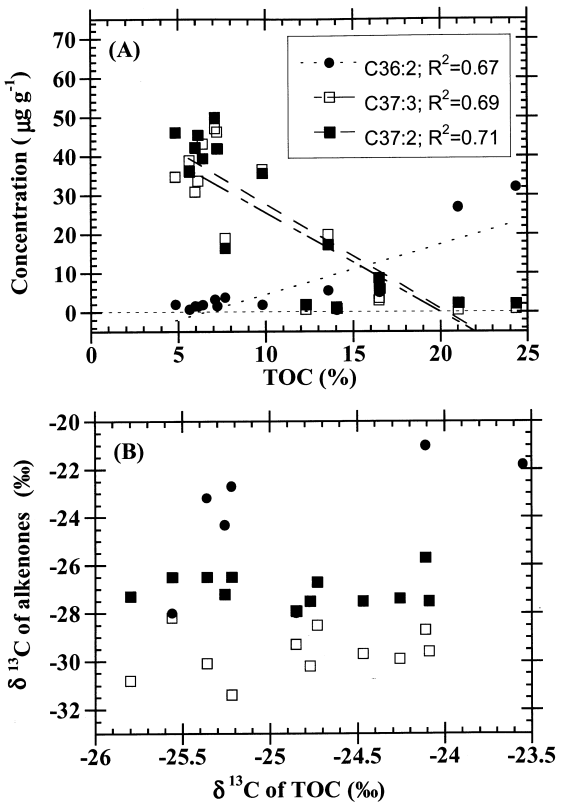

Fig. 9. Concentration of alkenones versus total organic carbon (A) and $\delta^{13}C$ of alkenones versus the $\delta^{13}C$ of TOC (B) in BC-17 sediments. Symbols used in Fig. 9A are the same as those in Fig. 9B.

The haptophytes *Gephyrocapsa oceanica* and *Isochrysis galbana* are known to be significant precursors for alkenones in coastal regions and could potentially represent a source of alkenones in the Black Sea (Marlowe et al., 1984b, 1990; Volkman et al., 1995; Conte et al., 1998). However, as for *E. huxleyi*, there are no published reports of a $C_{36:2}$ alkenone in these algae in culture. Overall, while we can only speculate about the biological source of the new compound, it seems clear that it has an origin that is distinct from the commonly observed di-, tri-, and tetraunsaturated C_{37} to C_{39} alkenones.

Future work should be directed at determining the biological source of this new compound and evaluating its impact on existing alkenone-based proxy records.

4. Conclusions

A novel alkenone in Black Sea sediments has been isolated from Black Sea Unit II sediments. After a series of chemical, GC, MS, NMR, and IR analyses, we have identified the new compound as hexatriaconta-(16*E*, 21*E*)-dien-3-one ($C_{36:2}$). Down-core variations in abundance and isotopic composition suggest that the precursor for the $C_{36:2}$ alkenone may be distinct from that of the $C_{37\text{-}39}$ alkenones, however the biological origin for this novel compound is presently unknown.

Acknowledgements

We thank Dr. Xuchen Wang, Ms. Leah Houghton, and Mr. Sean Sylva for MS analyses, and Mrs. Qingmei Lin and Dr. Kai Hinrichs for assistance in interpreting MS data. Mr. Mark Dennet and Dr. Joel Goldman are

thanked for the seed culture of *I. galbana*. Mr. Al Gagnon was an invaluable source of information on the sediment cores. We wish to thank Dr. Sidney Bourne (Bourne Scientific, Acton, MA, USA) and Professor Marc Lamontagne (Rhode Island College, RI, USA) for their generosity and assistance with the GC–IR and FT–IR measurements respectively. We thank Carles Pelejero and Gerard Versteegh as well as the associate editor for providing constructive comments on an earlier version of this manuscript. This research was funded by NSF Grants OCE-9809624 and OCE-9415568. L.X. is grateful for the scholarship provided by the China Scholarship Council. This is Woods Hole Oceanographic Institution contribution number 10419.

Associate Editor—**J. Volkman**

References

Arthur, M.A., Dean, W.E., 1998. Organic-matter production and preservation and evolution of anoxia in the Holocene Black Sea. Paleoceanography 13, 395–411.

Arthur, M.A., Dean, W.E., Neff, E.D., Hay, B.J., King, J., Jones, G., 1994. Varve calibrated records of carbonate and organic carbon accumulation over the last 2000 years in the Black Sea. Global Biogeochemical Cycles 8, 195–217.

Batchelor, J.G., Cushley, R.J., Prestegard, J.H., 1974. Carbon-13 Fourier transform nuclear magnetic resonance. 8. Role of steric and electric field effects in fatty acid spectra. Journal of Organic Chemistry 39, 1698–1705.

Bertsch, W., 2000. Two-dimensional gas chromatography concepts, instrumentation, and applications — Part 2: comprehensive two-dimensional gas chromatography. Journal of High Resolution Chromatography 23, 167–181.

Boon, J.J., van der Meer, F.W., Schuyl, P. J.W., de Leeuw, J.W., Schenck, P.A., Burlingame, A.L., 1978. Organic geochemical analyses of core samples from Site 362, Walvis Ridge. DSDP Leg 40. In: Initial Reports of the Deep Sea Drilling Project. Vol. 40. US Government Printing Office, Washington. pp. 627–637.

Brassell, S.C., Eglinton, G., Marlowe, I.T., Pflaumann, U., Sarnthein, M., 1986. Molecular stratigraphy: a new tool for climatic assessment. Nature 320, 129–133.

Bukry, D., 1974. Coccoliths as paleosalinity indicators — evidence from Black Sea. In: Degens, E.T., Ross, D.A. (Eds.), The Black Sea — Geology, Chemistry, and Biology. American Association of Petroleum Geologists, Oklahoma, pp. 353–362.

Christie, W.W., 1982. Lipid Analysis, 2nd Edition. Pergamon, England.

Conte, M.H., Thompson, A., Lesley, D., Harris, R.P., 1998. Genetic and physiological influences on the alkenone/alkenoate versus growth temperature relationship in *Emiliania huxleyi* and *Gephyrocapsa oceanica*. Geochimica et Cosmochimica Acta 62, 51–68.

Cranwell, P.A., 1985. Long-chain unsaturated ketones in recent lacustrine sediments. Geochimica et Cosmochimica Acta 49, 1545–1551.

Eglinton, G., Bradshaw, S.A., Rosell, A., Sarnthein, M., Pflaumann, U., Tiedemann, R., 1992. Molecular record of secular sea surface temperature changes on 100 year timescales for glacial terminations I, II and IV. Nature 356, 423–426.

Eglinton, T.I., Boon, J.J., Minor, E.C., Olson, R.J., 1996. Microscale characterization of algal and related particulate organic matter by direct temperature-resolved mass spectrometry. Marine Chemistry 52, 27–54.

Eglinton, T.I., Conte, M., Eglinton, G., Hayes, J., 2000. Alkenone biomarkers gain recognition as molecular paleoceanographic proxies. Eos 81, 253, 260.

Farrington, J.W., Davis, A.C., Sulanowski, J., McCaffrey, M.A., McCarthy, M., Clifford, C.H., Dickinson, P., Volkman, J.K., 1988. Biogeochemistry of lipids in surface sediments of the Peru upwelling area at 15°S. Organic Geochemistry 13, 607–617.

Freeman, K.H., Wakeham, S.G., 1992. Variations in the distributions and isotopic compositions of alkenones in Black Sea particles and sediments. Organic Geochemistry 19, 277–285.

Gaines, R.B., Frysinger, G.S., Hendrick-Smith, M.S., Stuart, J.D., 1999. Oil spill source determination by comprehensive two-dimensional gas chromatography. Environmental Science and Technololgy 33, 2106–2112.

Hay, B.J., Honjo, S., Kempe, S., Ittekkot, V.A., Degens, E.T., Konuk, T., Izdar, E., 1991. Sediment deposition in the Late Holocene abyssal Black Sea with climatic and chronological implications. Deep Sea Research Part A 38 (suppl. 2), S1237–S1254.

Gong, V., Hollander, D.J., 1999. Evidence for differential degradation of alkenones under contrasting bottow water oxygen conditions: Implications for paleotemperature reconstruction. Geochimica et Cosmochimica Acta 63, 405–411.

Jasper, J.P., Hayes, J.M., 1990. A carbon isotope record of CO_2 levels during the late Quaternary. Nature 347, 462–464.

Jasper, J.P., Hayes, J.M., Mix, A.C., Prahl, F.G., 1994. Photosynthetic fractionation of ^{13}C and concentrations of dissolved CO_2 in the central equatorial Pacific during the last 255,000 years. Paleoceanography 9, 781–798.

Johnson, C.G., Eglinton, T.I., Nelson, R.K., 1997. Determination of unsaturation ratios for long chain ketones by high resolution mass spectrometry. Proceedings of the 45th ASMS Conference on Mass Spectrometry and Allied Topics, Palm Springs, CA, p. 1383.

Jones, G.A., Gagnon, A.R., 1994. Radiocarbon chronology of Black Sea sediments. Deep-Sea Research Part I 41, 531–557.

Koopmans, M.P., Schaeffer-Reiss, C., de Leeuw, J.W., Lewan, M.D., Maxwell, J.R., Schaeffer, P., Sinninghe Damsté, J.S., 1997. Sulfur and oxygen sequestration of n-C_{37} and n-C_{38} unsaturated ketones in an immature kerogen and the release of their carbon skeletons during early stages of thermal maturation. Geochimica et Cosmochimica Acta 61, 2397–2408.

de Leeuw, J.W., van der Meer, F.W., Rijpstra, W.I.C., Schenck, P.A., 1979. On the occurrence and structural identification of long-chain unsaturated ketones and hydrocarbons in recent and subrecent sediments. In: Douglas, A.G., Maxwell, J.R. (Eds.), Advances in Organic Geochemistry 1979. Pergamon Press, New York, pp. 211–217.

Leonhardt, B.A., DeVilbiss, E.D., 1985. Separation and double-bond determination on nanogram quantities of aliphatic

monounsaturated alcohols, aldehydes and carboxylic acid methyl esters. Journal of Chromatography 322, 484–490.

Li, J., Philp, R.P., Pu, F., Allen, J., 1996. Long-chain alkenones in Qinghai Lake sediments. Geochimica et Cosmochimica Acta 60, 235–241.

Marlowe, I.T., Brassell, S.C., Eglinton, G., Green, J.C., 1984. Long chain unsaturated ketones and esters in living algae and marine sediments. Organic Geochemistry 6, 135–141.

Marlowe, I.T., Brassell, S.C., Eglinton, G., Green, J.C., 1990. Long-chain alkenones and alkyl alkenoates and the fossil coccolith record of marine sediments. Chemical Geology 88, 349–375.

Marlowe, I.T., Green, J.C., Neal, A.C., Brassell, S.C., Eglinton, G., Course, P.A., 1984. Long chain (n-C_{37}–C_{39}) alkenones in the Prymnesiophyceae. Distribution of alkenones and other lipids and their taxonomic significance. British Phycology Journal 19, 203–216.

McCaffrey, M.A., Farrington, J.W., Repeta, D.J., 1990. The organic geochemistry of Peru margin surface sediments–I. A comparison of the C_{37} alkenone and historical El Niño records. Geochimica et Cosmochimica Acta 54, 1671–1682.

McNichol, A.P., Osborne, E.A., Gagnon, A.R., Fry, B., Jones, G.A., 1994. TIC, TOC, DIC, DOC, PIC, POC-unique aspects on the preparation of oceanographic samples for ^{14}C-AMS. Nuclear Instruments and Methods in Physics Research B92 162–165.

Phillips, J.B., Beens, J., 1999. Comprehensive two-dimensional gas chromatography: a hyphenated method with strong coupling between the two dimensions. Journal of Chromatography, A. 856, 331–347.

Phillips, J.B., Gaines, R.B., Blomberg, J., Schoenmakers, P., van der Wielen, F.W.M., Dimandja, J.-M., Green, V., Granger, J., Patterson, D., Racovalis, L., de Geus, H.-J., de Boer, J., Haglund, P., Lipsky, J., Veena, S., Ledford, E.B., 1999. A robust thermal modulator for comprehensive two-dimensional gas chromatography. Journal of High Resolution Chromatography 22, 3–10.

Prahl, F.G., Wakeham, S.G., 1987. Calibration of unsaturation patterns in long-chain ketone composition for paleotemperature assessment. Nature 330, 367–369.

Prahl, F.G., Muehlhausen, L.A., Zahnle, D.L., 1988. Further evaluation of long-chain alkenones as indicators of paleoceanographic conditions. Geochimica et Cosmochimica Acta 52, 2303–2310.

Rechka, J.A., Maxwell, J.R., 1988a. Characterisation of alkenone temperature indicators in sediments and organisms. Organic Geochemistry 13, 727–734.

Rechka, J.A., Maxwell, J.R., 1988b. Unusual long chain ketones of algal origin. Tetrahedron Letters 29, 2599–2600.

Rieley, G., Teece, M.A., Peakman, T.M., Raven, A.M., Greene, K.J., Clarke, T.P., Murray, M., Leftley, J.W., Campbell, C.N., Harris, R.P., Parkes, R.J., Maxwell, J.R., 1998. Long-chain alkenes in haptophytes *Isochrysis galbana* and *Emiliania huxleyi*. Lipids 33, 617–625.

Sessions, A.L., Burgoyne, T.W., Schimmelmann, A., Hayes, J.M., 1999. Fractionation of hydrogen isotopes in lipid biosynthesis. Organic Geochemistry 30, 1193–1200.

Schouten, S., van Driel, G.B., Sinninghe Damsté, J.S., de Leeuw, J.W., 1993. Natural sulfurization of ketones and aldehydes: A key reaction in the formation of organic sulfur compounds. Geochimica et Cosmochimica Acta 57, 5111–5116.

Sinninghe Damsté, J.S., Rijpstra, W.I.C., Kock-van Dalen, A.C., de Leeuw, J.W., Schenck, P.A., 1989. Quenching of labile functionalised lipids by inorganic sulphur species: evidence for the formation of sedimentary organic sulphur compounds at the early stages of diagenesis. Geochimica et Cosmochimica Acta 53, 1343–1355.

Thiel, V., Jenisch, A., Landmann, G., Reimer, A., Michaelis, W., 1997. Unusual distributions of long-chain alkenones and tetrahymanol from the highly alkaline Lake Van, Turkey. Geochimica et Cosmochimica Acta 61, 2053–2064.

Thomsen, C., Schulz-Bull, D.E., Petrick, G., Duinker, J.C., 1998. Seasonal variability of the long-chain alkenone flux and the effect on the $U^{K'}_{37}$-index in the Norwegian Sea. Organic Geochemistry 28, 311–323.

Volkman, J.K., Barrett, S.M., Blackburn, S.I., Sikes, E.L., 1995. Alkenones in *Gephyrocapsa oceanica*: Implications for studies of paleoclimate. Geochimica et Cosmochimica Acta 59, 513–520.

Volkman, J.K., Eglinton, G., Corner, E.D.S., Forsberg, T.E.V., 1980a. Long-chain alkenes and alkenones in the marine coccolithophorid *Emiliania huxleyi*. Phytochemistry 19, 2619–2622.

Volkman, J.K., Eglinton, G., Corner, E.D.S., Sargent, J.R., 1979. Novel unsaturated straight-chain C_{37}–C_{39} methyl and ethyl ketones in marine sediments and a coccolithophorid *Emiliania huxleyi*. In: Douglas, A.G., Maxwell, J.R. (Eds.), Advances in Organic Geochemistry 1979. Pergamon Press, New York, pp. 219–227.

Wakeham, S.G., Sinninghe Damsté, J.S., Kohnen, M.E., de Leeuw, J.W., 1995. Organic sulfur compounds formed during early diagenesis in Black Sea sediments. Geochimica et Cosmochimica Acta 59, 521–533.